When steric hindrance facilitates processivity: polymerase activity within chromatin

Christophe BECAVIN, Jean-Marc VICTOR and Annick LESNE

Institut des Hautes Études Scientifiques
35, route de Chartres
91440 – Bures-sur-Yvette (France)

Octobre 2007

IHES/P/07/37

When steric hindrance facilitates processivity: polymerase activity within chromatin

Christophe Bécavin[(a)], Jean-Marc Victor[(b)], Annick Lesne[(a,b)]

(a) Institut des Hautes Études Scientifiques
Le Bois-Marie, 35 route de Chartres, 91440, Bures-sur-Yvette, France.
(b) Laboratoire de Physique Théorique de la Matière Condensée
Université Pierre et Marie Curie-Paris 6
4 place Jussieu, F-75252 Paris Cedex 05, France.

During eukaryotic transcription, polymerase activity generates torsional stress in DNA, having a negative impact in polymerase processivity. Using our previous studies of the chromatin fiber structure and conformational transitions, we suggest that this torsional stress can be alleviated thanks to a balance between fiber twist and a nucleosome conformational transition into a reversome state. Our model enlightens the origin of polymerase pauses, and leads to the counter-intuitive conclusion that chromatin organized compaction might facilitate polymerase processivity. Indeed, in a compact and well-structured chromatin loop, steric hindrance between nucleosomes enforce sequential transitions, thus ensuring that the polymerase always meets a permissive nucleosomal state.

Keywords: transcription, chromatin fiber, processivity, supercoiling, reversome, pauses

1 Introduction

Transcription is a fundamental biological process during which a dedicated protein, the RNA-polymerase (RNAP), achieves the synthesis of a RNA stretch from a genomic DNA template. Transcription can be divided into three steps: initiation, elongation and termination. Initiation provides RNAP with an access to the promoter sequence. In eukaryotes cells, this requires the assembly of trancription factors together with RNAP into the transcription initiation complex. We here do not address problems related to the initiation phase, which are by far the most complex ones, inasmuch as they are involved at the heart of the transcriptional regulation. We focus on the elongation phase, which starts once the elongation complex has been completed, and progresses until a termination sequence is encountered. The

elongation complex (EC) consists of a denaturation bubble of length about 10 nucleotides, enclosed within RNAP [1]. During elongation, RNAP tracks along the genomic sequence, 'swallowing' the DNA double helix.

However in eukaryotic species, genomic DNA is wrapped around octamers of histone proteins, forming nucleosomes in turn organized at a higher level into a chromatin fiber. This complex architecture is bound to hinder both the initiation and the elongation phases [2]. In the standard paradigm, transcription elongation requires a decondensed state of chromatin, namely euchromatin, to take place. This is questionable at least for two reasons:
(i) *in vivo*, chromatin decondensation remains elusive, all the more as chromosome structure is not yet elucidated. A central question to be addressed is: at which scale does decondensation occur? It is generally assumed that the fiber itself is decondensed in euchromatin, but the fiber structure has never been resolved, neither in euchromatin nor in heterochromatin - and we don't even know whether there is any difference between both structures;
(ii) *in vitro*, even in decondensed fibers, nucleosomes constitute nearly absolute blocks to RNA-polymerase progression [3].
We wish to examine here in which conditions elongation could take place within a *condensed* chromatin fiber, and if so, in which way. Moreover we will examine whether condensed structures could even be helpful.

2 Biological setting

Our approach is based on a modeling study of the interplay between conformational dynamics of the chromatin fiber and RNA-polymerase processing along the fiber [4]. It is rooted in experimental knowledge about transcription and its actors. We recall here the main biological features of eukaryotic transcription, while focussing on recent biophysical results.

2.1 RNAP or DNA: which is moving?

There are three types of RNAP according to the type of RNA they synthesize. RNAP I is dedicated to ribosomal RNAs (rRNAs) synthesis and occurs in a particular environment - the nucleolus - probably devoid of nucleosomes because of its very high transcription rate. RNAP II transcribes RNA encoding proteins. The corresponding transcripts, so-called mRNAs, are much longer than the transcripts delivered by RNAP III, i.e. tRNAs and other small RNAs. Entanglement problems are therefore much more stringent for RNAP II than for RNAP III. As a matter of fact, RNAP progression along the genomic sequence requires a relative rotation of the RNAP together with its transcript around the DNA. Then there are two possibilities: either the DNA is kept fixed and the RNAP turns around it, thus following the DNA helical groove and producing a RNA strand coiled around the DNA double

helix; or the RNAP is kept fixed and the DNA double helix has to screw inside it. In the first case, long RNA transcripts could be hardly untangled and processed further into a migrating mRNA. That is why we favor the second case, where the RNAP is anchored to some nuclear structure (*e.g.* transcription factory [5]).

2.2 The twin-supercoiled-domain model

This assumption implies in turn a topological problem because eukaryotic transcription occurs within chromatin loops [6], that is, partially decondensed regions of post-mitotic chromosomes, about 50 kilobases long and separated by boundaries. The loop ends are clamped by insulator elements [7], not necessarily tightly tethered to a matrix but enough constrained to make each loop an end-anchored stretch of DNA, that 'traps' DNA supercoiling and ensures the conservation of the linking number in the loop. We recall that the linking number is roughly the number of times one DNA strand is coiled around the other one [8]. It is a topological quantity, i.e. independent of the conformation of the loop, and is conserved in the absence of topoisomerase activity. As the elongation complex progresses along the genomic sequence, the DNA double helix in front of it becomes overwound (positively supercoiled) whereas the DNA behind it becomes underwound (negalively supercoiled), in a way that conserves the global linking number of the loop. This is the so-called twin-supercoiled-domain (TSD) model, first introduced by Liu & Wang [9] and extensively acknowledged since (for a review, see [10]).

2.3 Nucleosome conformations in a transcribing loop

The TSD model has been shown to be potentially relevant for eukaryotes as well [11, 12]. More recently Matsumoto and Hirose directly visualized (by fluorescence imaging) transcription-coupled negative supercoiling in chromatin even in the presence of active topoisomerases [13], thus strongly supporting the model. But what kind of structural rearrangement of the chromatin loop should occur jointly with the absorption of positive (resp. negative) supercoiling downstream (resp. upstream)? We recently revisited the TSD model in the chromatin context by means of a single chromatin fiber nanomanipulation by magnetic tweezers and we proposed that nucleosomes may act as a topological buffer [14]. Our scenario relies on the existence of three stable nucleosome states evidenced by the nanomanipulation, namely: N (negatively crossed), O (open), P (positively crossed), according to the relative position and orientation of the linkers one with respect to the other (see Fig. 1). We recall that these states had been previously characterized within minicircles (a minicircle is a single nucleosome within a closed stretch of DNA [15]). Note that in higher eukaryotes, linker histones H1/H5 presumably play a role both in stabilizing the states N and P against O, and channeling the transition in between them by acting as a pivot [16].

2.4 The reversome hypothesis

A convergent set of experimental observations [17, 18, 19] tends to indicate that RNAP II can transcribe through a nucleosome only if the nucleosome is in an activated conformation.

Using the same single molecule nanomanipulation (the same set-up), we found that a fiber submitted to a large positive torsional stress can trap positive turns at a rate of one turn per nucleosome. This trapping has been shown to reflect a nucleosome chiral transition to a metastable state, called reversome. This new state has been claimed to be a good candidate for the required activated conformation. Indeed, the transition to reversome is accompanied by the undocking of both H2A-H2B dimers from the (H3-H4)2 tetramer that relieves the block to RNAP progression.

One advantage of this auxiliary transcriptional mechanism is to avoid the need for a complete disassembling of the nucleosome into single histones, hence epigenetic labels (controlling *e.g.* the kinetics of initiation and elongation) can be preserved. The original fiber structure is fully restored right after the passage of the polymerase, allowing a new processing. Moreover, this conformational change modifies the linking number per nucleosome by an amount $\mathbf{L}^R - \mathbf{L}^N \approx 1$.

2.5 The fiber structure in a transcribing loop

After more than thirty years of effort, the structure of the chromatin fiber is still a matter of debate, mainly because it is not directly observable and varies considerably according to the cell cycle period and functional status of the fiber, with possibly several different structures coexisting along the chromosome [20]. The fiber structure is no better stated in a transcribing loop. This is precisely one of the questions we aim to answer with our modeling.

We shall here distinguish two structures differing in their degree of compaction: the decondensed fiber (with less than $\Lambda = 0.5$ nucleosome per nm along the fiber) and the condensed fiber (with more than $\Lambda = 0.5$ nucleosome per nm along the fiber). The condensed chromatin fiber is expected to have a regular structure since it is favored energetically (stacking interactions between nucleosomes) and possibly functionally, hence selected during (spontaneous) self-organization or (active) remodeling of the fiber. It has been shown in vitro that a small amount of nucleosome positioning is enough to get a regular structure [21]. Accordingly, we shall consider as the generic setting the regular model structure of chromatin fiber established in a previous work. This structure presents a strong nucleosome stacking hence strong steric hindrance [22].

3 Our modeling framework

Let sum up here the biological bases of our modeling of transcription elongation in a chromatin loop:

(i) The RNAP is anchored to some nuclear structure and exerts a torque inducing the rotation of DNA on itself (uncoiling of the double helix) that can be estimated from experimental data to occur at a constant rate of $\omega_0 = 4\pi$ rad/s (2 turns per second) [23]. This rotation at a constant rate of the first DNA linker provides a first boundary condition in our modeling; what happens upwards and downwards is precisely the question we aim to answer.
(ii) The DNA is screwing inside the RNAP, inducing positive (resp. negative) supercoiling in the downstream (resp. upstream) part of the loop.
(iii) The positive torque exerted by RNAP onto the loop has to induce the transition of nucleosomes to reversomes so as to allow the progression of the RNAP.
Typical values of the relevant parameters of the model are sum up in table I.

We will adopt a field-theoretic effective modeling of the fiber as an homogeneous elastic rod [24] as discussed below in Section 4.2, and consider two alternative scenarios according to the degree of compaction of the fiber. Our modeling will appreciate the role of chromatin fiber rigidity, the transmission of the torque exerted by RNAP along the fiber and the dissipation in the surrounding viscous medium. We shall also investigate the role of nucleosome conformations and conformational changes, in particular their impact on topological constraints. From a functional and evolutionary viewpoint, one might expect the response of the chromatin fiber to be coupled to the RNAP activity in such a way that the ensuing feedback loop at the same time promotes and regulates transcriptional elongation.

Our framework thus lies at the crossing of *elasticity theory*, here of a one-dimensional medium, that is an elastic rod[25], *Kramers theory* to compute rate constants from the knowledge of the energy landscape [26], and *reaction-diffusion theory* to bridge the local conformational changes (the 'reaction') with mechanical propagation of the stresses and strains (the 'diffusion'), here moreover globally constrained by topological conservation laws.

Entity	Parameter	Typical value	Definition
RNAP	ω_0	4π rad/s	angular velocity induced by RNAP to DNA (or equivalently to the fiber)
	V	20 bps/s	RNAP velocity, *i.e.* number of transcribed bps per second
Loop	$\mathcal{N}$	250	number of nucleosomes per chromatin loop
	L_0	250–1250 nm	loop length
	l_0	100–500 nm	length of the loop region downwards the initiation site
Fiber	Λ	0.2–1 nm^{-1}	linear density of nucleosomes in a fiber
	$\mathcal{L}_p$	30–300 nm	persistence length of the fiber
DNA	l_{pitch}	3.4 nm	pitch of the DNA-double helix in B-form
	n_{pitch}	10.5 bps	number of base pairs corresponding to the pitch
Nucleosome	n_{repeat}	200 bps	nucleosome repeat length, *i.e.* number of bps per nucleosome
	l_{repeat}	70 nm	length of DNA per nucleosome $l_{repeat} = n_{repeat}.l_{pitch}$
	$\mathbf{L}^P - \mathbf{L}^N$	1	linking number difference (per nucleosome) between negative (N) and positive (P) states
	$\mathbf{L}^R - \mathbf{L}^P$	1	linking number difference (per nucleosome) between positive (P) and reversome (R) states

Table I. Biological setting. Summary of the notations and typical values of the parameters.

4 Preliminary investigations: several time and space scales

A fruitful guideline for an efficient modeling is to identify the space and time scales of the different elementary processes involved in the polymerase and fiber functional dynamics. It then allows to exploit scale separation, if any, to implement quasi-stationary approximations and associated decouplings in order to reduce the dimensionality of the relevant model.

4.1 Polymerase motion

We shall denote x the arc-length (curvilinear abscissa) measured along the chromatin fiber, with $x > 0$ downwards the polymerase, located by definition in $x = 0$ (see Fig. 2). A length Δx along the chromatin fiber corresponds to a length $\Delta x \, \Lambda \, l_{repeat}$ along the embedded DNA where $l_{repeat} \approx 70$ nm is the repeat length, that is, the DNA length per nucleosome; it equivalently corresponds to a number $\Delta x \, \Lambda \, n_{repeat}$ of base pairs, where $n_{repeat} \approx 200$ bps is the number of bps per nucleosome. For instance, with $\Lambda = 1$ nm^{-1}, a length $\Delta x = 1$ nm corresponds to about

200 bps. The length of the chromatin loop downwards the polymerase is

$$l(t) = l_0 - X(t) \tag{1}$$

where $X(t)$ is the distance traveled by the polymerase (see Fig. 2), measured along the fiber (x-axis), that is

$$X(t) = \frac{\omega_0\, t\, l_{pitch}}{2\pi\, \Lambda\, l_{repeat}} \tag{2}$$

where $l_{pitch} = 3.4$ nm is the pitch of the DNA double helix, hence[1]

$$X(t) = Vt \quad \text{with} \quad V = \frac{\omega_0\, l_{pitch}}{2\pi\, \Lambda\, l_{repeat}} \approx 10^{-10}\,\mathrm{m/s} \tag{3}$$

We anticipate that the polymerase velocity V is far smaller than the propagation of the torsional stress along the chromatin fiber. We shall present in this Section 4 the validation of this important working hypothesis, since it will justify a quasi-stationary (also called 'adiabatic') approximation, according which the instantaneous state of the fiber (*e.g.* profiles of strains, stresses and local conformational changes, if any) is computed as a quasi-equilibrium state while considering that the position of the polymerase is fixed; the displacement $t \to X(t)$ is plugged in the obtained formulas only in a second and decoupled stage of the computation.

4.2 Chromatin fiber effective modeling

At the relevant spatial scale, namely that of a chromatin loop of length $L_0 \approx 1\mu$m along the fiber axis, we can adopt a continuous-medium description and consider the chromatin fiber as an *elastic rod* [24, 25]. To be valid, this framework mainly requires to describe the fiber behavior at the level of a few nucleosomes, with an elementary length dx along the fiber axis such that $1/\Lambda \ll dx \ll \mathcal{N}/\Lambda$; this amounts to smooth out single-nucleosome inhomogeneities and to describe the average fiber behavior at a supra-nanometer scale. This continuous description is supported by the high and regular density of nucleosomes Λ varying between 0.2 and 1 nm^{-1} (number per nm along the fiber axis). We shall denote $\tau(x,t)$ the twist rate of the fiber and $\mathcal{L}_p$ its twist persistence length. The value of $\mathcal{L}_p$ is about 30 nm in a decondensed fiber and presumably larger, up to 300 nm, in a tightly condensed fiber because of steric hindrance [28]. In this setting, the local state of the fiber is described by means of one or more continuous deterministic fields $\Phi(x,t)$ as, for instance, the fiber torsional shear (denoted Γ below) or the local nucleosome state (denoted ξ below). Actually Φ accommodates only an average and continuous description of the fiber features, namely an *homogenized* description of the fiber architecture and local state: its discrete nucleosomal structure is somehow spread uniformly over a

[1] The polymerase is a motor protein able to rectify thermal fluctuations so as to achieve an oriented motion; as such, its velocity is a well-defined quantity, independent of the spatial scale at which it is considered, in contrast to a mere Brownian particle.

region dx of a few nm along the fiber axis, corresponding to a few repeat lengths along the DNA; any information about the relative 3-dimensional positioning, if it is to be taken into account (for instance a change in the fiber radius) should be introduced as an additional field component.

Structural inhomogeneities might be taken into account as *disorder*, but in a first step, we favor the most parcimonious model with the least number of adjustable parameters, so as to get the most stringent test of validity of the underlying scenario. Actually, DNA-sequence effects self-average at the fiber scale, supporting still more an homogenized model. Such an approach implicitly assumes some scale separation insofar as it is expected that molecular details, here up to the nucleosome scale, can be accounted for through effective parameters in a higher-scale model, here a continuous model at the fiber scale. Conversely, feedbacks of the fiber structure and dynamics on the nucleosome level or below are expected to be fully encapsulated, as regards their consequences on both the fiber behavior and nucleosome state, through the value of a local field Φ (coupled to the fiber local order parameter and acting as a forcing term or external influence in the nucleosome state equation or conformational dynamics) [29].

4.3 Propagation of torsional stress in a semi-infinite fiber

Let us suppose that the polymerase is fixed in $x = 0$. A preliminary issue is to investigate the propagation of the torsional stress generated by the polymerase in a *semi-infinite* chromatin fiber (that is, with no end-constraint downwards). At the chromatin scale, inertia effects can be ignored hence it is relevant to restrict to the *over-damped regime*, in which external forces and torques are fully balanced by viscous dissipation. Introducing the twist rate $\tau(x,t)$ and the integrated twist rate $\Theta(x,t) = \int_0^x \tau(z,t)dz$, such that $\Theta(x,t)$ is the angle by which a fixed point on the chromatin fiber surface at abscissa x has turned around the fiber axis at time t, it comes:

$$\frac{\partial \Gamma}{\partial x}(x,t) = -\,\eta\, R^2 \frac{\partial \Theta}{\partial t}(x,t) \tag{4}$$

where $\Gamma(x,t)$ is the local torque, $(\partial\Gamma/\partial x)(x,t)$ the net torque experienced by an element dx of the elastic rod of radius $R \approx 15$ nm modeling the chromatin fiber, and $\eta \approx 10^{-3}$ N.s.m^{-2} the dynamic viscosity of the surrounding solvent (water or crowded chromatin, but in any case, η does not overwhelm ten times the viscosity of pure water). For the typical stresses and strains generated by the polymerase, it is legitimate to work within linear response theory and to consider that the local torque is proportional to the differential strain (*i.e.* torsional shear):

$$\Gamma(x,t) = -\,kT\,\mathcal{L}_p\,\tau(x,t) = -\,kT\,\mathcal{L}_p\,\frac{\partial \Theta}{\partial x}(x,t) \qquad \text{since} \quad \tau(x,t) = \frac{\partial \Theta}{\partial x}(x,t) \tag{5}$$

where k is the Boltzmann constant and T the temperature. Jointly, these two equations lead to a plain diffusion equation for $\Theta(x,t)$:

$$\frac{\partial\Theta}{\partial t} = D\frac{\partial^2\Theta}{\partial x^2} \qquad \text{where} \quad D = \frac{kT\,\mathcal{L}_p}{\eta\,R^2} \tag{6}$$

yielding $D \approx 1.8\ 10^{-10}$ m^2/s for $\mathcal{L}_p \approx 30$ nm. Derivation of (6) with respect to x (resp. t) leads to the same diffusion equation for $\tau(x,t)$ (resp. $(\partial\Theta/\partial t)(x,t)$); derivation of (4) with respect to x and (5) with respect to t leads to the same diffusion equation for $\Gamma(x,t)$. The boundary conditions are on one side $(\partial\Theta/\partial t)(x=0,t) \equiv \omega_0$ and $(\partial\Gamma/\partial x)(x=0,t) \equiv -\eta\,R^2\,\omega_0$, where $\omega_0 \approx 4\pi$ rad/s is prescribed by the polymerase activity, and on the other side, $\tau(x\to\infty,t) \equiv 0$ hence $\Gamma(x\to\infty,t) \equiv 0$ and $(\partial\Theta/\partial t)(x\to\infty,t) \equiv 0$. Taking into account these boundary conditions, integration of the diffusion equation for $\partial\Theta/\partial t$ leads to:

$$\frac{\partial\Theta}{\partial t}(x,t) = \omega_0\left[1 - erf\left(\frac{x}{\sqrt{4Dt}}\right)\right] \tag{7}$$

where $erf(\,.\,)$ is the error function ($erf(0)=0$ and $erf(x\to\infty)=1$) and

$$\Gamma(x,t) = \omega_0\,\eta\,R^2\left[x\cdot erf\left(\frac{x}{\sqrt{4Dt}}\right) - x + \sqrt{Dt}\cdot e^{-x^2/4Dt}\right] \tag{8}$$

The scaling form of this expression means that the strain spreads along the fiber roughly as $\sqrt{4Dt}$; in other words, the interplay between rotational viscosity and fiber rigidity produces an effective diffusive spreading. It thus takes $t_0 \sim l_0^2/4D \approx 2.10^{-3}$ s (or even less, roughly $t_0' \approx 2.10^{-4}$ s, for the upper bound $\mathcal{L}_p' \approx 300$ nm) for the strain to invade the length of a loop, whereas the polymerase progresses by 4.10^{-3} turn, that is, 0.04 bp, during this time (or even less than 10^{-2} bp in a more rigid compact fiber, in which the correlation between local strains is stronger). Thus, *a posteriori*, the time scales of the described phenomena, compared to that of the polymerase motion along the fiber, validate the quasi-stationary approximation made in investigating the fiber behavior while considering that the polymerase is fixed in $x=0$. We have only to plug in all the results the relation $x = \tilde{x} - X(t)$ between the absolute position $\tilde{x}$ along the fiber and the distance x to the polymerase (*i.e.* the position in a frame moving with the polymerase, see Fig. 2).

In this simple model of the polymerase/fiber mechanical interplay, the torque takes its maximal value right downwards the polymerase, and this maximal value $\Gamma(0,t)$ increases with time without bound like $\sqrt{Dt}$, meaning that torsional stress accumulates right ahead the polymerase as transcription takes place. This feature shows that the polymerase cannot process simply like that, and a more sophisticated scenario, involving a conformational change within the fiber, strain exchange and ensuing stress relaxation is required. Moreover, polymerase transcriptional activity occurs within a chromatin loop, so that torsional strain cannot escape to infinity hence is trapped unless some topoisomerases enter the scene. It makes the impeding influence of the strain on the polymerase progression and the requirement of alleviating it all the more stringent.

4.4 A hierarchy of separated scales

In conclusion, we have shown, without any specific assumption on the fiber structure nor on the nucleosome conformation, that at least three well-separated time scales can be identified in transcription elongation:

(i) the propagation of the torsional strain in the whole chromatin loop (without any conformational change) takes place at a fast scale, about 10^{-3} s;

(ii) the central time scale is that of the relaxation of torsional constraint and elastic strain relying on nucleosome-reversome transitions, and leading to a 'transient' quasi-equilibrium state;

(iii) finally, the slowest time scale is that of polymerase progression along the fiber: the polymerase takes roughly 10 s to pass the 200 bps corresponding to the DNA length per nucleosome.

(iv) Moreover, a fourth time scale is that of the nucleosome conformational change triggered by the torsional constraints generated by the polymerase activity, that will be described in the next Section 5. Its location in the above hierarchy is a priori unclear and will be central to the alternative modeling assumptions discussed in Section 6.

5 Chromatin loop response to polymerase activity

5.1 Mechanical control of the nucleosome-reversome transition

The nucleosome conformational change, at the relevant functional time scales, can be described within the framework of chemical kinetics. Considering a free-energy landscape (Fig. 1) with three minima N, P and R, corresponding respectively to three nucleosome states with $F_R > F_P \approx F_N$, and a maximum B corresponding to the top of the barrier encountered during the transition between states P and R, Kramers theory is well-suited to compute the rate constant k of the transition $P \to R$, the rate constant k' of the reverse transition $R \to P$, and the equilibrium constant $K = k'/k$ [26]. Note that the transition from a negative nucleosome (state N) to the reversome (state R) necessarily begins with the transition from N to P. Our focus is here on the influence of torsional constraints $\Gamma(x,t)$ experienced by the chromatin fiber onto these rate constants. The relevant framework to include the mechanical contribution to free energy is generalized thermodynamics (thermodynamic of elastic media that parallels thermodynamics of dielectric or magnetic media). Namely, the relevant landscape for applying Kramers theory is now

$$G = F - 2\pi \mathbf{L}\Gamma \tag{9}$$

where $\Gamma(x,t)$ is the torque experienced by the fiber at time t and point x and $\mathbf{L}(x,t)$ is the local contribution to the linking number of the fiber, simply related to the DNA one according to [8]

$$\mathbf{L}^{DNA} = \mathbf{L}^{fiber} - \frac{n(t)}{n_{pitch}} \tag{10}$$

where $n_{pirtch} = 10.5$ is th number of base pairs in a DNA pitch and $n(t)$ is the number of base pairs in the downward part of the loop at time t.

The key point is the following: whereas the reversome state is a meta-stable state in an unconstrained fiber, with $F_R > F_P$, it becomes the privileged state in an enough constrained fiber since $G_R < G_P$ for $\Gamma > \Gamma^* = (F_R - F_P)/2\pi(\mathbf{L}^R - \mathbf{L}^P)$. Indeed, the forward rate constant writes $k(\Gamma) = k_0\, e^{-(G_B - G_P)/kT}$, the backward rate constant $k'(\Gamma) = k_0\, e^{-(G_B - G_R)/kT}$ and the equilibrium constant

$$K(\Gamma) = e^{-(G_P - G_R)/kT} = e^{-2\pi(\mathbf{L}^R - \mathbf{L}^P)(\Gamma - \Gamma^*)/kT} \tag{11}$$

Accounting for the fact that $\mathbf{L}^R - \mathbf{L}^P \approx +1$ and using the measured value $F_R - F_P \approx 6kT$ [30], it simply comes:

$$K(\Gamma) = e^{-2\pi(\Gamma - \Gamma^*)/kT} \qquad \text{where} \quad \Gamma^* = \frac{3kT}{\pi} \tag{12}$$

The threshold value Γ^* of the torque, hence the equilibrium constant $K(\Gamma)$, are independent of the barrier B between the two nucleosomal states P and R and only depend on the difference between their respective free energies whereas the barrier height controls the transition kinetics.

A side remark is to be done to complete the above reasoning: since $F_P \approx F_N$ whereas $\mathbf{L}^P - \mathbf{L}^N \approx +1$, the slightest torsional constraint makes the positive state P of the nucleosome highly favored. Since moreover the bare energy barrier between N and P is low, the torsional constraint exerted by the polymerase will begin to switch all negative nucleosomes, if any, to the positive state (either at random in the decondensed fiber or in a row due to steric constraint in the condensed fiber, see below models A and B). This will absorb a given amount of supercoiling, according to the number of negative nucleosomes in this part of the loop. This switch occurs quite fast compared to the time required to observe the transition $P \to R$, hence it could be considered as a transient, preliminary step. We might henceforth start the investigation of the transition towards an activated reversome state at the moment where all downward nucleosomes are in the positive state.

5.2 Topological constraint trade-off

In naked DNA, the DNA linking number conservation expresses in a balanced interchange between DNA twist and plectoneme formation (DNA writhe). Within a chromatin fiber loop, whose writhe is negligible (less than 0.01 per nucleosome [8]),

a different trade-off will take place between chromatin fiber twist and nucleosome conformational transitions, first from negative to positive state then, once all nucleosomes have switched to P state (by convention at time $t = 0$), from positive state P to reversome R. In the adopted continuous-medium description, it is relevant to introduce a smooth field $\xi(x,t)$ representing the fraction of reversomes at time t and point x along the fiber. The linking number of the fiber being equal to that of the DNA composing it, up to a constant [8] (see Eq. (10), the conservation of stored elastic strain writes:

$$\mathbf{L}^{(fiber)}(t) - \mathbf{L}^{(fiber)}(0) = \int_0^{l(t)} \left[\frac{\tau(x,t)}{2\pi} + \Lambda(\mathbf{L}^R - \mathbf{L}^P)\xi(x,t) \right] dx = \frac{\omega_0 t}{2\pi} \qquad (13)$$

We recognize on the right-hand-side of (13) the sum of the total twist $\Theta[l(t),t]$ and the contribution of all the transitions into the reversome state that have occurred in the loop at time t. As the transition $P \to R$ proceeds, the total twist of the loop decreases by one unit (one turn) for each transition. Equations (4) and (5) are still valid, and Θ, Γ, τ and all their derivatives still satisfy the diffusion equation (6). But now the boundary conditions are prescribed in an implicit and under-determined way, via the integral equation (13) that involves the unknown field $\xi(x,t)$. In other words, the driving exerted by the polymerase expresses as a constraint on the *integrated* quantity $\mathbf{L}^{(fiber)}(t)$, hence $d\mathbf{L}^{(fiber)}/dt = \omega_0/2\pi$. By contrast to the case of a semi-infinite fiber with no nucleosome conformational change, (13) no longer constrain $(\partial\Theta/\partial t)(0,t)$ (differing from Eq.(7), yielding $(\partial\Theta/\partial t)(0,t) = \omega_0$). In particular, a locally homogeneous solution for Γ, with $(\partial\Gamma/\partial x)(0,t) \equiv 0$ and accordingly $(\partial\Theta/\partial t)(x = 0,t) \equiv 0$, is no longer excluded; it would correspond to a (locally) constant profile for Γ hence a linear profile for Θ. In view of the continuous increase of the integral constraint, we expect the profile $\Gamma(x,t)$ to rise monotonously in time at each fixed x, but cannot at this stage determine its shape and explicit evolution.

5.3 Two alternative closures

In order to fully exploit the conservation equation (13) and get explicit boundary conditions for $\Gamma(x,t)$ and $\Theta(x,t)$, a closure relation is needed, that relates $\xi(x,t)$ to the other unknown quantities. It will depend on the dominant mechanism controlling the spatial distribution of the global trade-off between fiber twist and nucleosome transition to reversome. Hence, introducing this closure relation will rely on some additional understanding or assumption regarding the whole functional process and not only the local physical aspects described above. Basically, two alternative models and associated closure relations can be considered. They correspond to two instances of the $P \to R$ transition, determined by the degree of compaction and organization of the fiber. In a decondensed fiber (model A), the transition will take place at random positions in the downward region $[0, l(t)]$ of the fiber, according to a (chemical) equilibrium distribution. In a condensed fiber (model B), due to steric constraints,

the transition will occur in a sequential way within a localized layer propagating in front of the polymerase.

6 Model A: transcription within a decondensed fiber

In a decondensed fiber, the actual kinetic rate of the nucleosome transition $P \rightarrow R$ are simply those established in Subsection 5.1 on thermodynamic grounds; the associated characteristic times support a quasi-stationary approximation where the transition from nucleosome to reversome is supposed to reach instantaneously its equilibrium at each place and time:

$$\xi(x,t) = \xi_{eq}[\Gamma(x,t)] = \frac{1}{1+K[\Gamma(x,t)]} \tag{14}$$

Plugging in the expression (11) of the equilibrium constant yields:

$$\xi_{eq}[\Gamma] = \frac{1}{1+e^{-2\pi(\Gamma-\Gamma^*)/kT}} = \frac{1+\tanh\left(\frac{\Gamma-\Gamma^*}{\Delta\Gamma}\right)}{2} \tag{15}$$

where we read $\Delta\Gamma = \frac{kT}{\pi}$, corresponding to the width of the profile $\Gamma \rightarrow \xi(\Gamma)$, while Γ^* (we recall that $\Gamma^* = 3kT/\pi$) corresponds to the inflection point, with $\xi = 1/2$ for $\Gamma = \Gamma^*$ (see Fig. 3). We here identify three time scales:
— the fast scale of the relaxation of ξ to the equilibrium profile $\xi_{eq}[\Gamma]$, with a time scale $\sup(1/k, 1/k')$;
— the central scale at which the profile $\Gamma(x)$ evolves in response to a change in $\mathbf{L}^{(DNA)}$;
— the slow scale of the polymerase motion (change by two turns per second of $\mathbf{L}^{(DNA)}$).

$\xi(x,t)$ also represents the probability for a nucleosome to be in a reversome upon imposing one additional turn. It is maximal near the polymerase, decreases monotonously with x, and remains non-vanishing in the whole chromatin loop. From the biological viewpoint, the flaw of this model is that $\xi(0,t)$ will markedly depart from 1, meaning that the polymerase does not necessarily face a reversome during its progression along the fiber, which is inconsistent with its activity since it cannot transcribe through a nucleosome. Hence model A fails to reproduce the chromatin context required for polymerase processing and continued transcription, and we have to reconsider the associated premise of transcription occurring in a decondensed fiber.

7 Model B: transcription within a condensed fiber

In this second model, we consider polymerase activity within a condensed fiber. The most relevant feature of the fiber structure [22] is then the *regular and close nucle-*

osome stacking into helical piles (or starts[2]), see Fig. 4. The closeness of stacked nucleosome faces along the start axis generates geometric constraints on the conformational changes of a single nucleosome. For instance, the conversion of a single nucleosome into a reversome within a stacked pile is prevented due to steric hindrance, that not only reinforces the energy penalty of a configuration PRP along the pile, compared to PPP or RRR, but imposes a transient opening and reorganization of the pile for the transition to occur, that is simply forbidden. Nucleosome stacking thus favors an all-or-none behavior, reminiscent of a domino effect[3].

The fiber response to the torsional constraint imposed by the polymerase activity is now controlled by the direct interaction between the border layer of the reversome front and the adjacent layer of stacked nucleosomes, and essentially by what happens in the linker relating the most downward reversome and the following nucleosome: here is the basic step in the propagation of the mechanical constraints that trigger the transition of the latter one and stabilize the reversome state of the former one, in an irreversible way. Model B thus describes a situation where steric constraints prevent the relaxation to chemical equilibrium and actually maintain the fiber in a far-from-equilibrium state[4].

This qualitative analysis leads to assume, as a closure relation, that steric hindrance between successive nucleosomes in each column enforces a sequential transition along the fiber, hence a step-like profile (see Fig. 5):

$$\xi(x,t) = 1 \quad \text{for } x \leq x^*(t), \text{ else } 0 \qquad \text{and } \Gamma = \Gamma^* \text{ for } x \leq x^*(t), \text{ else } 0 \tag{16}$$

As expressed in (13), the transition $P \to R$ absorbs some part of the supercoiling (or equivalently the fiber supercoiling) but some fiber twist has to be present to maintain the torque Γ at the threshold value Γ^*. Spatial homogeneity of the torque Γ implies the constancy of the spatial rate

$$\tau(x,t) \equiv \tau^* = \frac{\Gamma^*}{kT\,\mathcal{L}_p} = \frac{3}{\pi\,\mathcal{L}_p} \quad \text{for } x \leq x^*(t) \tag{17}$$

[2]The axis of the helical starts being by definition transverse to the dyad axis of the stacked nucleosomes, there is only one way of decomposing the 30nm-fiber into a bunch of a variable number n of nucleosomal piles: one thus speaks of *n-start fiber structure* [22].

[3]Such cooperativity is typically observed in multi-subunits allosteric enzymes, the most acknowledged example being hemoglobine and its 'umbrella opening': the conformational change of a single subunit is associated with a so strong disorganization of th overall structure that the subunit conformational transitions occur jointly, or not at all. Symmetries of the original and final superstructures play a central role in enforcing cooperativity, for both steric and energetic reasons. In the chromatin fiber, two symmetries are involved in coordinating $P \to R$ transition: the stacking of nucleosomes along helical piles wrapped around the fiber axis in a n-start fiber; the lateral interaction of these columns enforced by their intricate and alternate wrapping around one and the same axis that promotes regularity and homogeneity; single nucleosome conformational transitions appear as prohibitive isolated 'defects'.

[4]The oriented progression of the transition front raises no puzzle as regards to the Second Principle of thermodynamics: it is induced by the oriented and active boundary condition. In other words, it simply reflects the oriented, non equilibrium activity of the polymerase and its remote downstream consequences, propagated by the chromatin semi-rigid structure.

from which we compute the contribution $x^*(t)\Gamma^*/\mathcal{L}_p\,kT$ of the fiber twist to the total linking number, supplementing the contribution $\Lambda x^*(t)$ of all the transitions $P \to R$ that have occurred between $x = 0$ and $x = x^*(t)$. We finally obtain:

$$\frac{\omega_0\,t}{2\pi} = x^*(t)\left(\Lambda + \frac{\Gamma^*}{kT\mathcal{L}_p}\right) \quad \text{hence} \quad x^*(t) = \frac{\omega_0\,t}{2\pi(\Lambda + 3/\pi\mathcal{L}_p)} \approx \frac{\omega_0\,t}{2\pi\Lambda} \tag{18}$$

Since $\tau^* \ll 1/\Lambda$, the supercoling is almost fully absorbed into the transitions, whereas the part contributing to the fiber twist is almost negligible, as long as the transitions $P \to R$ proceed, that is, as long as $x^*(t) < l(t)$. This yields a time threshold

$$t < t^* = \frac{2\pi\,l_0\,\Lambda}{\omega_0 + 2\pi\,\Lambda\,V} \tag{19}$$

with a numerical value around 50 s. At $t = t^*$, the whole downward chromatin loop is composed of reversomes and any additional DNA supercoiling turns into fiber twist; the torque increases rapidly, soon becoming too strong to be overcome and the polymerase stops, what is seen as a pause in transcription.

The polymerase motion monitors the evolution of the profile $\xi(x,t)$: each time the polymerase has advanced by $\delta x = l_{pitch}/\Lambda\,l_{repeat} \approx 1/20$ nm along the fiber and accordingly increased $\mathbf{L}^{(DNA)}$ *i.e.* $\mathbf{L}^{(fiber)}$ by one turn, the reversome front has progressed by one nucleosome $\Delta x = 1$ nm. The step velocity is related to the polymerase velocity according to $dx^*/dt = (l_{repeat}/l_{pitch})\,V \approx 20\,V \approx 2$ nm/s. It is very slow and viscous effects can be ignored. The polymerase progresses in a slower way, since V is about 20 times slower than the propagation of the reversome step. The conservation of the total linking number of the loop, *i.e.* the region between the two topological boundaries, implies that nucleosomes turn progressively to the negative state in the wake of the polymerase (region $x < 0$) to compensate the supercoiling induced by the polymerase in the downward part (region $x > 0$), see Fig. 5.

The biologically important feature is that all the reversomes are in a row in front of the polymerase, hence the step profile associated with model B is the most efficient: it achieves twist relaxation and at the same time ensures that the polymerase progresses in a locally open and transcriptionally permissive configuration, encountering only 'transparent' reversomes.

8 Biological interpretation and predictions

8.1 Model A vs model B

The models A and B both led to physically consistent behavior. They express the following alternative: RNAP processing within a decondensed fiber without stacking interactions nor steric hindrance between successive nucleosomes (model A) or within a condensed chromatin fiber (model B). They can be discriminated

only on biological grounds, namely the requirement for the processing polymerase to encounter only nucleosomes in an activated state identified with the reversome state. The main distinction between models A and B comes from a geometric argument: in model B, steric constraints prevent the chemical equilibrium to be reached (a kind of frustration phenomenon) and enforce the sequential transition of nucleosomes into reversomes. We favor model B against model A since in the latter, the polymerase would still encounter nucleosomes blocking its progression.

8.2 A local chromatin fiber decondensation

We are thus led to the following quite counter-intuitive prediction: polymerase processivity is favored in a compact chromatin fiber (model B) since then, steric constraints between nucleosomes enforce a step-like reversome profile ensuring that the polymerase will always be faced to reversomes during its progression. In other words, polymerase activity within a compact fiber modifies its surroundings in such a way as to ensure that each nucleosome encountered by the polymerase as it moves along the fiber will be in the reversome conformation. The spreading of the reversome phase in model B appears as a *precursor* extending farther and farther ahead of the processing polymerase, and moving about twenty times faster than the polymerase[5].

There is no need for a full decondensation of the chromatin fiber to accommodate transcription elongation. The loop decondensation indirectly observed in vivo in yeast [31], where a chromatin locus moves towards a nuclear pore upon transcription, presumably takes place at a higher level, that of chromonemes [32], composed of compact chromatin fiber, either folded or unfolded . Arguably, only the local decondensation associated with the conformational change of nucleosomes into reversomes is required for polymerase processing. It is nevertheless to underline that we here consider only the elongation phase; a local decondensation of the 30nm-fiber is required for the transcription initiation.

8.3 An essentially active and topology-driven process

The system is driven by the polymerase activity, imposing a certain 'angular velocity' (a twist rate) ω_0. Spreading of the elastic constraints and conformational changes is thus essentially different from a reaction-diffusion front, spontaneously propagating once proper initial conditions are met. Whereas other aspects of the system are shared by mere mechanical objects or soft matter, this intrinsic internal driving reflects the active processes at work and corresponds to a biological specificity, encountered only in living or artificial systems. In consequence, the relevant conservation laws are not the dynamic ones (there is *e.g.* no momentum conservation) not even energy conservation (it is an active process continuously fed by

[5]Similar to the propagation of a front and its precursor: Kessler, D.A., Ner, Z. and Sander, L.M. (1998) Front propagation: Precursors, cutoffs, and structural stability, *Phys. Rev. E* **58**, 107–114.

ATP flux, that is, chemical energy), but *conservation of topological invariants*. Viscous effects also are negligible at the chromatin fiber scale: the numerical value of D (a rotational diffusion coefficient) shows that only crowding and end-anchoring, generating topological constraints, are sufficient to prevent the free rotation of the fiber.

8.4 Predictions and plausible explanations of some RNAP features

Confronting our scenario and its predicted observable consequences with experimental data would give clues about the fiber structure and conformational rigidity and cooperativity. Since structure and conformational dynamics of the fiber are not directly observable in vivo, any indirect clue about these structure and dynamics and their role in major biological processes like transcription would be of high value. In particular, the processes described in this paper show that strong inhomogeneities in the fiber structure appear as topological defects and could play the role of boundaries as regards wave propagation or topological constraints; here they would prevent the propagation of the $P \rightarrow R$ transitions and associated facilitation of polymerase activity.

Our model suggests that the decondensation required for transcription elongation to take place concerns only higher levels of organization, beyond the chromatin level. It predicts that RNAP processing would be less efficient, if not impossible, in decondensed chromatin fiber.

As soon as all the nucleosomes have turned into reversomes, the additional supercoiling exerted by the polymerase fully accumulates in the form of fiber twist, and the strain rapidly becomes too strong for the polymerase to process any more, and a pause of the transcriptional activity is observed. Our model thus predicts that polymerase pausing will occur soon after the reversome front has reached the loop boundary, *i.e.* when $t = t^*$, while the polymerase has traveled $X_{max} \sim l_0/20$. It leads to the rough estimate that pauses will occur after polymerase has processed 10 nm of fiber, that is, 1 kbp, corresponding to a duration between 25 s and 100 s of processive activity. Moreover, noting that the torsional constraint is $\mathbf{L}^{(DNA)} - \int_0^{l(t)} \Lambda(\mathbf{L}^R - \mathbf{L}^P)\xi(x,t)dx$ whereas it would be $\mathbf{L}^{(DNA)}$ without any nucleosome/reversome transition, in particular for polymerase processing naked DNA, we expect pauses to be far more frequent within naked DNA (*e.g.*, as observed in nano-manipulations of polymerase on naked DNA [33], or in prokaryotes [34]) than in vivo, within a chromatin context.

9 Conclusion

Based on the facts that polymerase transcribes only through an activated nucleosome state and its processing modifies the DNA linking number, we have proposed

a scenario elucidating how transcription elongation can proceed within chromatin. At odds with current views, this scenario does not require a decondensation of the 30nm-fiber. Our modeling study of the interplay between the RNA-polymerase activity and the chromatin fiber conformational dynamics evidences that, on the contrary, the presence of steric, mechanical and topological constraints enforce an ordered pre-activation of the fiber downwards the polymerase. More precisely, within a condensed fiber loop with closely stacked nucleosomes, the very polymerase activity and the torsional constraints it generates in the chromatin fiber trigger the propagation of a conformational transition of the nucleosomes into a transcription-prone structure, more permissive to RNA-polymerase processing and transcriptional activity; we identify this nucleosomal structure with a recently proposed 'reversome' conformation. In a decondensed fiber, these nucleosome transitions would occur at random positions in the loop and it would require an unrealistic long time before the downward chromatin has been turned into a transcriptionally permissive substrate in which polymerase could proceed.

The plausibility of the proposed scenario is supported by several functional advantages. Conformational changes of the chromatin fiber and polymerase processing are tunable and never out of control: any factor-induced or sequence-induced defect in the chromatin fiber prevents the nucleosome transition to reversome and blocks the polymerase activity; conversely, the spreading of strain and ensuing conformational changes of the nucleosomes stops as soon as the polymerase activity stops. Fiber organization and steric hindrance between stacked nucleosomes appear to have a positive impact in channeling and ordering otherwise stochastic events, ensuring a greater efficiency of the polymerase activity and an increased robustness of transcription. This scenario relies on the interplay between different levels of organization, different space and time scales, local regulation and global timing, coupling between genetic and epigenetic information processing. It offers an explicit example of epigenomics since the polymerase processing could easily be controlled at the chromatin fiber level, *e.g.* via some post-translational histone modifications or cofactor binding preventing the transition to reversome. The reversome front propagation results from a driven reaction-diffusion mechanism, where the diffusive term originates in a short-range mechanical coupling between stacked nucleosomes; it is an instance of the fiber allosteric behavior we have already underlined to be a central feature in the functional role of the fiber [29]. Here constraints generated by the polymerase propagate and trigger a remote effect (the transition$P \rightarrow R$) thanks to topological invariants and nucleosome stacking: importantly, such allosteric potentialities are present only in a condensed loop.

Time-scale analysis has shown that dynamics is irrelevant, insofar as both inertia and viscous effects can be ignored in describing fiber functional processes: it is enough in a first stage to consider a sequence of quasi-equilibrium steps monitored by kinematic and topological constraints. Since this feature arises from the scale separation between molecular events and the chromatin fiber level, it is likely to be encountered for most processes occurring within the chromatin fiber and involving

its structural and topological properties. Finally, let us underline that it is a general fact that topological constraints induce long-range couplings along the fiber that coordinate fiber transactions and processes at the scale of a chromatin loop (typically embedding exons and introns associated to one gene); topological invariants play a channeling role in strongly constraining the possible deformations of the fiber. Conversely, functional constraints strongly condition the structure and dynamics of the fiber. Presumably, chromatin structure and function have co-evolved so as to reach a good, if not optimal, consistency and efficiency.

References

[1] Shilatifard, A., Conaway, R.C., and Conaway, J.W. (2003) The RNA polymerase II elongation complex, *Annual Review of Biochemistry* **72**, 693-715.

[2] Orphanides, G. and Reinberg, D. (2000) RNA polymerase II elongation through chromatin, *Nature* **407**, 471-475.

[3] Chang, C.H. and Luse, D.S. (1997) The H3/H4 tetramer blocks transcript elongation by RNA polymerase II in vitro, *J. Biol. Chem.* **272**, 23427-23434.

[4] Wolffe, A.P. (1998) *Chromatin: Structure and function*, Academic Press.

[5] Cook, P.R. (1999) The organization of replication and transcription, *Science* **284**, 1790-1795.

[6] Byrd, K. and Corces, V.G. (2003) Visualization of chromatin domains created by the gypsy insulator of Drosophila, *J. Cell Biol.* **162**, 565-574.

[7] Labrador, M. and Corces, V.G. (2002) Setting the boundaries of chromatin domains and nuclear organization, *Cell* **111**, 151-154.

[8] Barbi, M., Mozziconacci, J., and Victor J.M. (2005) How the 30 nm chromatin fiber deals with topological constraints, *Phys. Rev. E* **71**, 031910.

[9] Liu, L. F. and Wang, J. C. (1987) Supercoiling of the DNA template during transcription, *Proc. Natl. Acad. Sci. USA* **84**, 7024-7027.

[10] Lavelle, C. (2007) Transcription elongation through a chromatin template, *Biochimie* **89**, 519-527.

[11] Giaever, G.N. and Wang, J.C. (1988) Supercoiling of intracellular DNA can occur in eukaryotic cells, *Cell* **55**, 849-856.

[12] Ljungman, M. and Hanawalt, P.C. (1992) Localized torsional tension in the DNA of human cells, *Proc. Natl. Acad. Sci. USA* **89**, 6055-6059. Erratum in *Proc. Natl. Acad. Sci. USA* **89**, 9364.

[13] Matsumoto, K. and Hirose, S. (2004) Visualization of unconstrained negative supercoils of DNA on polytene chromosomes of Drosophila, *J. Cell Sci.* **117**, 3797-3805.

[14] Bancaud A. Conde e Silva, N., Barbi, M., Wagner, G., Allemand, J.F., Mozziconacci, J., Lavelle, C., Croquette, V., Victor, J.M., Prunell, A., and Viovy, J.L. (2006) Structural reorganization of single chromatin fibers revealed by torsional manipulation, *Nat. Struct. Mol. Biol.* **13**, 444-450.

[15] Sivolob, A., Lavelle, C., and Prunell, A. (2003) Sequence-dependent nucleosome structural and dynamic polymorphism. Potential involvement of histone H2B N-terminal tail proximal domain, *J. Mol. Biol.* **326**, 49-63.

[16] Sivolob, A. and Prunell, A. (2003). Linker histone-dependent organization and dynamics of nucleosome entry/exit DNAs, *J. Mol. Biol.* **331**, 1025-1040.

[17] Kireeva, M. L., Walter, W., Tchernajenko, V., Bondarenko, V., Kashlev, M. and Studitsky, V. M. (2002) Nucleosome remodeling induced by RNA polymerase II: loss of the H2A/H2B dimer during transcription, *Mol. Cell* **9**, 541-542.

[18] Lee, M. S. and Garrard, W. T. (1991) Positive DNA supercoiling generates a chromatin conformation characteristic of highly active genes, *Proc. Natl. Acad. Sci. USA* **88**, 9675-9679.

[19] Bondarenko, V. A., Steele, L. M., Ujvari, A., Gaykalova, D. A., Kulaeva, O. I., Polikanov, Y. S., Luse, D. S. and Studitsky, V. M. (2006) Nucleosomes can form a polar barrier to transcript elongation by RNA polymerase II, *Mol. Cell* **24**, 469-479.

[20] Van Holde, K. and Zlatanova, J. (2007) Chromatin fiber structure: Where is the problem now?, *Semin. Cell Dev. Biol.*, http://dx.doi.org/10.1016/j.semcdb.2007.08.005

[21] Weidemann, T., Wachsmuth, M., Tewes, M., Rippe, K. and Langowski, J. (2003) Counting nucleosomes in living cells with a combination of fluorescence correlation spectroscopy and confocal imaging, *J. Mol. Biol.* **334**, 229-240.

[22] Wong, H., Victor, J.M., and Mozziconacci, J. (2007) An all-atom model of the chromatin fiber containing linker histones reveals a versatile structure tuned by nucleosomal repeat length, *PLoS One*, **2**(9): e877. doi:10.1371/journal.pone.0000877

[23] Uptain, S.M., Kane, C.M., Chamberlin, M.J. (1997) Basic mechanisms of transcript elongation and its regulation, *Annu. Rev. Biochem.* **66**, 117-172.

[24] Ben-Haim, E., Lesne, A., and Victor, J.M. (2001) Chromatin : A tunable spring at work inside chromosomes, *Phys. Rev. E* **64**, 051921.

[25] Love, A.E.H. (1944) *Treatise on the mathematical theory of elasticity theory*, Dover.

[26] Gammaitoni, L., Hänggi, P., Jung, P., and Marchesoni, F. (1990) Reaction rate theory: fifty years after Kramers, *Rev. Mod. Phys.* **62**, 251-342.

[27] Daban, J.R. (2000) Physical constraints in the condensation of eukaryotic chromosomes. Local concentration of DNA versus linear packing ratio in higher-order chromatin structures, *Biochemistry* **39**, 3861-3866.

[28] Mergell, B., Everaers, R. , and Schiessel, H. (2004) Nucleosome interactions in chromatin: Fiber stiffening and hairpin formation, *Phys. Rev. E* **70**, 011915.

[29] Lesne, A. and Victor, J.M. (2006) Chromatin fiber functional organization: some plausible models, *Eur. Phys. J. E* **19**, 279–290.

[30] Bancaud, A. Wagner, G., Conde e Silva, N., Lavelle, C., Wong, H., Mozziconacci, J., Barbi, M., Sivolob, A., Le Cam, E., Mouawad, L., Viovy, J.L., Victor, J.M., and Prunell, A. (2007) Nucleosome chiral transition under positive torsional stress in single chromatin fibers, *Mol. Cell* **27**, 135-147.

[31] Cabal, G.G., Rodriguez-Navarro, S., Genevesio, A., Olivo-Marin, J.C., Zimmer, C., Gadal, O., Feuerbach-Fournier, F., Lesne, A., Buc, H., Hurt, E.C., and Nehrbass, U. (2006) Molecular analysis of SAGA mediated nuclear pore gene gating activation in yeast, *Nature* **441**, 770-773.

[32] Belmont, A.S., Dietzel, S., Nye, A.C., Strukov, Y.G., and Tumbar, T. (1999) Large-scale chromatin structure and function, *Curr. Opin. Cell Biol.* **11**, 307-311.

[33] Adelman, K., La Porta, A., Santangelo,T.J., Lis, J.T., Roberts, J.W. and Wang, M.D. (2002) Single molecule analysis of RNA polymerase elongation reveals uniform kinetic behavior, *Proc. Natl. Acad. Sci. USA* **99**, 13538-13543.

[34] Tolić-Nørrelykke, S.F., Engh, A.M., Landick, R., and Gelles, J. (2004) Diversity in the rates of transcript elongation by single RNA polymerase molecules, *J. Biol. Chem.* **279**, 3292-3299.

Contents

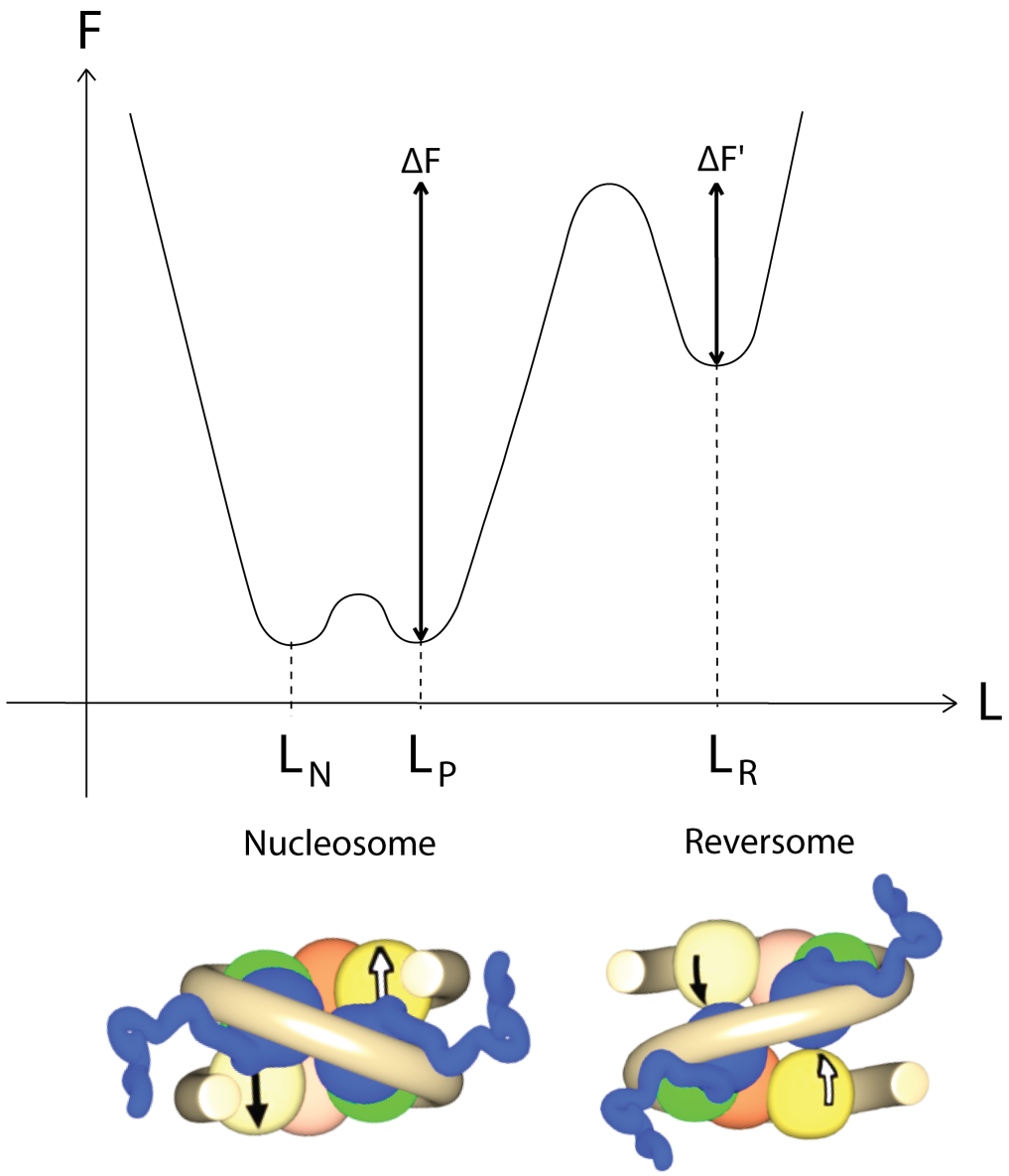

Figure 1: Free-energy landscape for the nucleosome conformation. The reaction coordinate (abscissa **L**) is the linking number of nucleosomal DNA; this choice appears relevant to investigate the landscape changes when a torque Γ is applied to the DNA, see section 4.1. Below are sketched the two main states: the current nucleosome, with two sub-states N and P according to the relative positions of the linkers (negative or positive crossing) and an activated state, the reversome, in which the histone core partially unfolds and the nucleosomal DNA adopts a right-handed path around the histone core. *Courtesy of Hua Wong.*

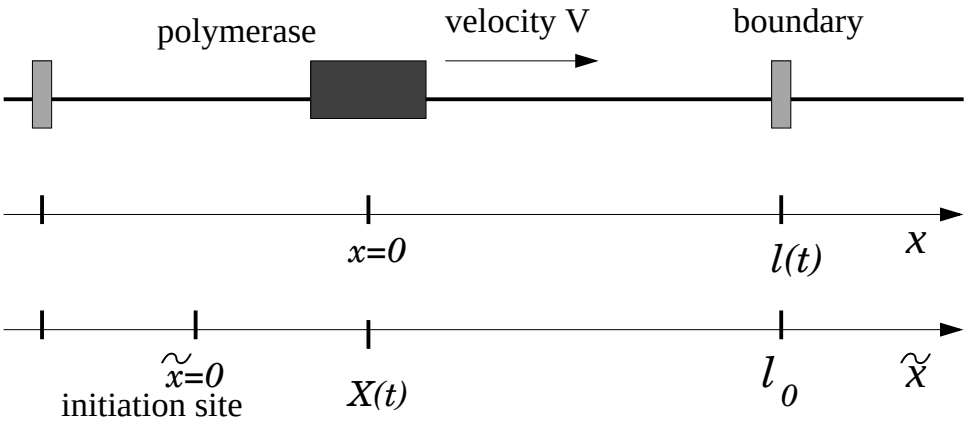

Figure 2: Relative (x) and absolute ($\tilde{x}$) positions along the chromatin fiber. The polymerase moves to the right, $X(t)$ being its position at time t. l_0 is the length of the loop region downwards the initiation site $X(0) = 0$ and $l(t) = l_0 - X(t)$ is the length remaining at time t between the polymerase and the downward boundary.

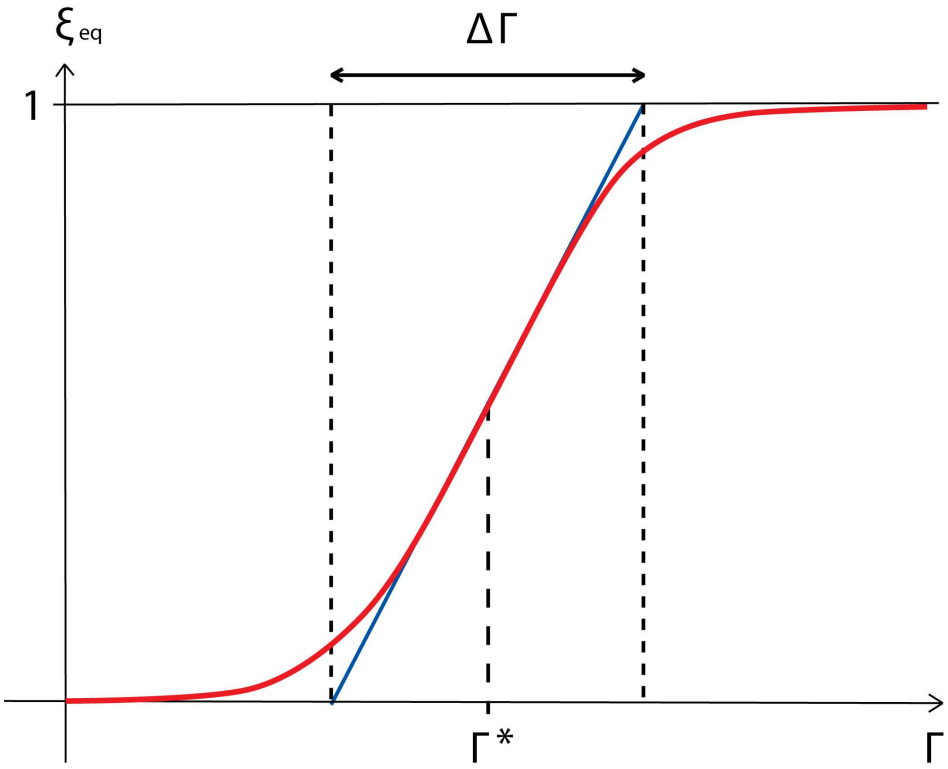

Figure 3: Reversome density ξ_{eq} as a function of the applied torque Γ when the transition between nucleosome and reversome states has reached its equilibrium, equation (15), with $\Gamma^* = 3kT/\pi$ and $\Delta\Gamma = kT/\pi$.

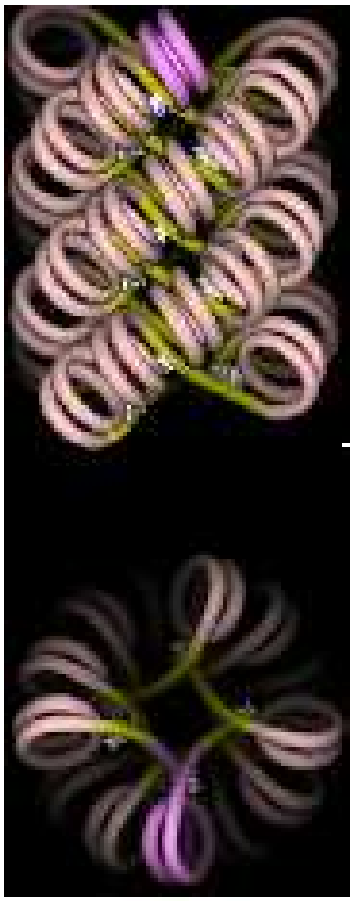

Figure 4: n-start fiber structure (with $n = 4$, corresponding to a repeat length of $n_{repeat} = 187$ bps) [22]. Notice the close and regular nucleosome stacking along each start, preventing the transition to reversome of a single nucleosome and rather enforcing a concerted sequential transition. *Courtesy of Julien Mozziconacci.*

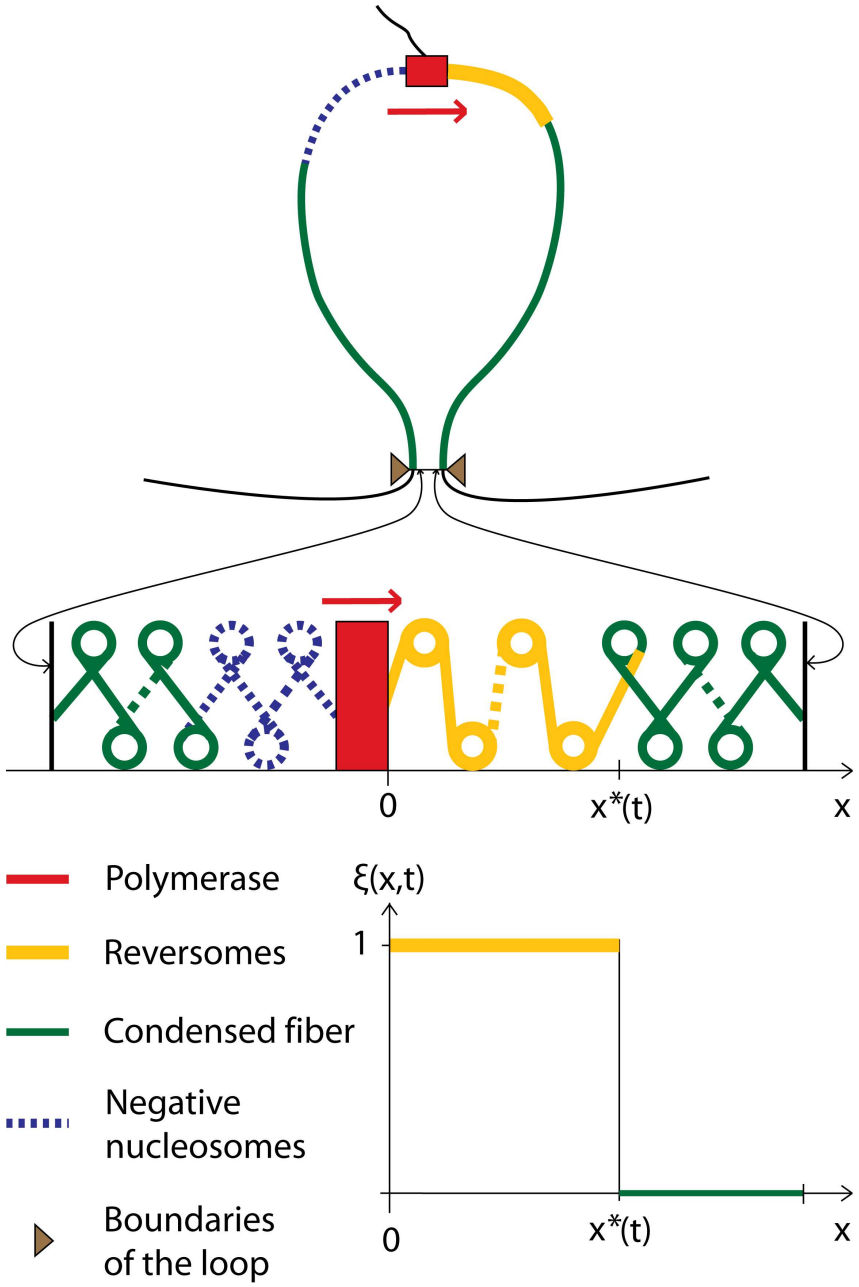

Figure 5: RNA-polymerase processing within condensed chromatin fiber. The supercoiling generated by the polymerase activity is trapped within the loop delineated by topological boundaries (the dashed black regions are outside the loop). The ensuing torsional constraints trigger the sequential transition of nucleosomes into reversomes (bold yellow region $[0, x^*]$, where the reversome density $\xi(x,t)$ equals 1) thus inducing a precursor permissive to RNAP processing. This precursor propagates downwards about 20 times faster than the polymerase progression. I the polymerase wake, the nucleosome turn to the negative state to ensure the conservation of the total linking number of the loop.